PCCP

Accepted Manuscript

ROYAL SOCIETY OF CHEMISTRY

www.rsc.org/pccp

Journal Name

ARTICLE TYPE

Cite this: DOI: 10.1039/xxxxxxxxxx

Dynamics of a plasmon-activated p-mercaptobenzoic acid layer deposited over Au nanoparticles using time-resolved SERS†

Gina Smith,‡ Jean-Sébastien Girardon, Jean-François Paul and Elise Berrier*

Received Date
Accepted Date

DOI: 10.1039/xxxxxxxxxx

www.rsc.org/journalname

Time-dependent SERS intensity recorded over a drop-coated coffee-ring pattern of p-MBA with gold colloids was investigated as a function of the specific laser power applied. Pure electromagnetic enhancement produced stochastic intensity variations of the whole SER spectra, which was mainly correlated to evolutions of the background intensity. Besides long-term, non-reversible spectral changes caused by plasmon-induced decarboxylation of p-MBA, transient original spectral profiles showing additional lines were also observed as the specific power reached $5.5 \times 10^4\,\mathrm{W\,cm^{-2}}$. An unprecedented qualitative and quantitative study of SERS intensity variations based on the complementary use of both extreme deviation and cross-correlation statistics is provided, which resulted in an improved understanding of SERS mechanisms. More precisely, cross-correlation analysis made it possible to follow the evolution of groups of modes assigned to one species or sharing same symmetry while so called individual events denote particular resonance structures, which occurrence was tentatively related to a photo-thermally activated motion of the gold nanostructures.

1 Introduction

Surface-Enhanced Raman Scattering (SERS) is nowadays a well-established technique for the detection of analytes which have an extremely low concentration [1,2]. The plasmonic excitation required for yielding a significant enhancement of the local electric field can also favour chemical reactions, which are essentially activated by thermal dissipation in the vicinity of the active nanostructure within a time scale of a nanosecond [3]. The *in situ* investigation of nanoparticle (NP)-catalysed and/or plasmon-activated chemical reactions using SERS seems to be a quite favourable entry to the depiction of reaction intermediates at the very surface of the active phase [4,5]. In this respect, a recent review by Harvey and Weckhuysen has paved the way to a strengthened use of SERS and TERS as *operando* probes for understanding heterogeneous catalytic processes [6].

Surface enhancement is related to two distinct mechanisms: the electromagnetic enhancement (EME) and the chemical enhancement (CE). EME is consistent with the local amplification of the electric field at one analyte molecule position [7] and was proposed to have no particular influence on the relative intensities of the observed modes [8]. Fluctuations of the EME are thus related to the ability of the probe molecule to reach a "hot spot" on one hand and the geometry of the nanostructure on the other hand. CE can arise from molecular excitation resonance, charge-transfer resonance and non-resonant changes in the molecule polarizability [9]. In the latter, the enhancement factor is highly dependent on the vibrational mode, the symmetry, the orbital involved in the charge-transfer process and, more generally, the chemical nature of the group interacting with the SERS substrate [10].

Temporal fluctuations of SERS intensity of CO adsorbed on gold roughened surfaces were reported by Kudelski and Pettinger [11] which were assigned to the structural modification of CO adsorption sites, *ie.* from top sites to bridging ones, as was quite recently also demonstrated by Wang *et al.* [12]. The use of confocal Raman spectroscopy makes it possible to selectively detect molecules adsorbed onto a limited number of "hot spots" and, hence, get information on the thermally activated diffusion of a limited number of molecules. This was the case in the temporal SERS fluctuations of Fungal Hypha reported by Szeghalmi *et al.* [13]. Hydrogenated amorphous carbon deposited on silver also gave rise to time-dependent strong variations of SERS signal from both qualitative and quantitative point of views [14]. Moreover, those fluctua-

Univ. Lille, CNRS, Centrale Lille, ENSCL, Univ. Artois, UMR 8181 - UCCS - Unité de Catalyse et Chimie du Solide, F-59000 Lille, France

† Electronic Supplementary Information (ESI) available: [Optical picture of coffee ring pattern, conventional Raman spectrum of p-MBA, SERS spectra presented as contour plot and waterfall for $P_S = 2.3 \times 10^5$ and $5.5 \times 10^4\,\mathrm{W\,cm^{-2}}$, covariance plot of Series recorded at $P_S = 2.3 \times 10^5\,\mathrm{W\,cm^{-2}}$ and Figure devoted to support discussion on spectral comb]. See DOI: 10.1039/b000000x/

‡ Present address: School of Chemistry, University of Edinburgh, Joseph Black Building, David Brewster Road, Edinburgh, Scotland EH9 3JJ.

* Corresponding author: Elise.Berrier@univ-lille1.fr

tions were shown by Kudelski to be quenched by the presence of chemisorbed anions[14], which suggests that the temporal fluctuations are due to a CE mechanism. Bizzarri and Cannistraro have proposed a statistical analysis of SERS intensity variations of the Fe-protoporphyrin:Ag system by means of covariance analysis[15]. More precisely, the authors have highlighted the role of background fluctuations on one hand and the variation of vibrational mode intensity produced by CE on the other hand. On the same system, some modes were shown to undergo an on/off switching behaviour and follow a Lévy statistics[16]. Finally, a very interesting work was quite recently published by van Schrojenstein Lantman *et al.* aiming at discriminating the rapid SERS intensity fluctuations from the time-resolved follow-up of the photocatalytic reduction of p-nitrophenol to p,p'-dimercaptoazobisbenzene using multivariate curve resolution (MCR) tools. A special attention was paid to the analysis of q-residuals, which specifically highlighted short-term deviation of the signal[17].

In this contribution, we investigate the fluctuation of SERS signals of para-mercaptobenzoic acid (p-MBA or 4-MBA), one of the most popular and common SERS probe. The SERS signature of p-MBA as well as the adsorption modes were thoughtfully investigated in the last decade by means of theoretical and experimental studies[18–25]. The consistency and complementarity of those reports serve as a basis for the in-depth investigation of the SER spectra of p-MBA.

2 Methods

2.1 Sample preparation

2.1.1 Synthesis of gold nanoparticles

A solution of gold colloids was prepared according to the Turkevich procedure[26]. Briefly, 12.5 mL of $HAuCl_4$ (5.4 mmol L^{-1}) was added to 213 mL of milli-Q water and stirred at 75 °C. The temperature was subsequently increased until the temperature reached 80 °C. 25.0 mL of sodium citrate (5.4 mmol L^{-1}) were added, so that the value of the cit:Au molar ratio is 2. The role of citrate was to both reduce the Au^{3+} ions and stabilize the NPs produced. Then the solution was heated for a further 30 minutes at 80 °C. The solution produced became increasingly coloured upon heating. The solution was subsequently allowed to cool down and stored in the dark at room temperature until required.

2.1.2 Drop coating deposition

150 μL of an aqueous solution of p-MBA (Aldrich) (10^{-4} mol L^{-1}) were mixed with 150 μL of citrate-Au colloids solution. This mixture was left for 2 hours to allow for possible reaction. A drop of the mixture was then deposited over a clean microscope slide, allowed to dry in ambient conditions and stored in the dark for several days at ambient temperature before being investigated. The resulting deposit had adopted the form of a so-called coffee-ring pattern containing an array of gold nanoparticles (AuNPs) covered by p-MBA. The SERS intensity was checked to be highest at the contour line of the pattern[27]. Because of the rather long contact time between the gold colloids and the p-MBA solution in both liquid and dried states, it was expected that if possible, catalytic reactions of p-MBA with AuNPs had occurred before the SERS analyses. Finally, it should be noted that no conventional Raman signal could be obtained with a coffee drop pattern prepared with the solution of p-MBA with no addition of AuNPs.

2.2 SERS analyses

SER spectra were recorded using a He-Ne laser for excitation (632.8 nm), the power at the sample was adjusted using neutral density filters for the purpose of the experiments. The laser beam was focused on the contour line of the coffee-ring pattern of sample using a 100X microscope objective (NA 0.9). The Raman signal was collected in backscattering mode using the same objective through a confocal hole of 150 μm. The scattered light was dispersed via a spectrometer equipped with a 600 grooves grating (typical spectral resolution at 632.8 nm: 6 cm^{-1}) and finally analysed using a Peltier-cooled CCD (Horiba Labram HR). The analysis was consistent with the collection of a series of SER spectra for 10 minutes using different laser powers at the sample. Depending on the acquisition time, each series gathered from 60 to 600 spectra. Unless otherwise stated, the analysed zone was changed for each series, and the very first spectrum of each series was verified to be rigorously identical to the others.

3 Results and Discussion

3.1 SER spectra of p-MBA:AuNPs as a function of the specific power applied to the sample, P_S

In order to get a general picture of the effects of P_S on the properties of the SER spectra, we present in Figure 1 the mean SERS signal afforded by averaging all spectra of the series recorded as a function of P_S.

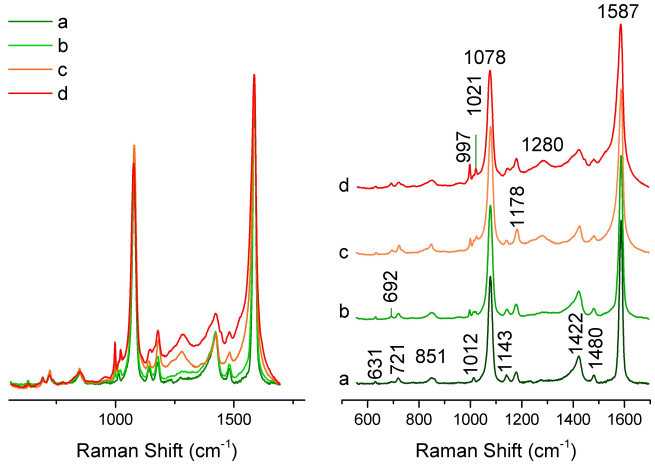

Fig. 1 Averaged and normalized SER spectra recorded using a specific power of a) 5.5×10^3 W cm^{-2}, b) 5.5×10^4 W cm^{-2}, c) 1.0×10^5 W cm^{-2} and d) 2.3×10^5 W cm^{-2}

In general, the increase of the specific power produces an increase of the background signal between 1000 and 1650 cm^{-1} (Figure 1, left side). The latter is an intrinsic phenomenon in SERS and can originate from both EME and CE[28]. The mean SER-averaged spectrum recorded with $P_S = 5.5 \times 10^3$ W cm^{-2} is similar in every respect to the profile of p-MBA adsorbed on silver or gold nanostructures at basic pH[18]. At first, the absence of the $\delta(CSH)$

bending mode expected at 910 cm^{-1} reflects, as expected, the adsorption of p-MBA by forming Au-thiolate bonds[29]. The main peaks located at 1078 and 1587 cm^{-1} are due to ν_{12} and ν_{8a} in plane vibrations of the benzene ring, respectively. The broad line around 1420 cm^{-1} is related to $\nu_s(COO^-)$[18,22]. Carboxylate groups also give rise to a bending mode vibration $\delta(COO^-)$ of moderate intensity observed at 851 cm^{-1}. The relative intensities of $\nu_s(COO^-)$ and $\delta(COO^-)$ were proposed by Suh *et al.* to be related to the geometry of the surface adsorbed carboxylate group[30]. The spectra we present here exhibit a $I_{\nu_s(COO^-)}$ significantly higher than $I_{\delta(COO^-)}$, indicating that, on average, p-MBA would adsorb onto the Au colloids surface with a tilted-flat orientation[18,30]. On the base of these results, one cannot exclude that the carboxylate groups could also interact with the gold surface.

Increasing P_S to 5.5×10^4 $W cm^{-2}$ produced the emergence of sharp features of weak intensity at 997 and 1021 cm^{-1} together with an increase of the contribution around 1570 cm^{-1}, which partly overlaps the ν_{8a} mode of p-MBA. These three lines were demonstrated by Zong *et al.* to reflect the presence of mono-substituted benzene derivatives produced by a plasmon-activated decarboxylation of p-MBA. The resulting species are thus similar in every respect to thiophenol adsorbed on a rough silver electrode[20]. Moreover, broad bands centred around 1300 and 1600 cm^{-1}, which could denote the formation of polycyclic aromatic hydrocarbons, come out as the specific power reaches 1.0×10^5 $W cm^{-2}$.

3.2 Temporal evolution of SERS intensity

3.2.1 Evolution of the intensity of SERS at low specific power (6×10^3 $W cm^{-2}$)

In order to afford an exploitable signal-to-noise ratio, the acquisition time was, in this case, set to 5 s. Spectral acquisitions were run every 10 s, so that a rest time of 5 s was applied between 2 acquisitions. Along the series of 60 spectra we have recorded, the intensity of the Raman signal is rather stable*. The first and last spectra are absolutely not distinguishable after normalizing their intensity with regards to their respective area. This trend indicates that no irreversible chemical change has occurred. Moreover, no spectrum of the series was found to feature any noticeable peculiarity.

3.2.2 Evolution of the intensity of SERS measured using a specific power of 5.5×10^4 $W cm^{-2}$

A similar experiment with $P_S = 5.5 \times 10^4$ $W cm^{-2}$ was run with an acquisition time of 0.5 s and an interval of 1 s between two spectra. In general, the integrated spectral intensity, presented in Figure 2a, was found to slightly decrease with time. On the other hand, some points featuring exceptionally high or low area values come out of the mean evolution presented in Figure 2. After having subtracted the spectra by means of a linear baseline, and thus, removed the continuous background emission from the SER spectra, the spectral area was stable and clear of exceptional values (Figure 2b). A standard deviation of ~4% was found, which is consistent with the experimental noise. As a result, both short and long-term variations of the overall SERS intensity essentially reflected changes of the background level.

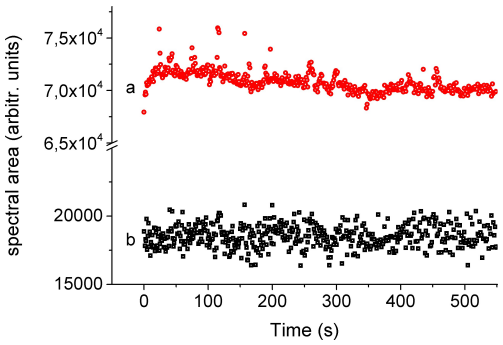

Fig. 2 Area of SER a) raw and b) baseline-subtracted spectra of MBA:Au deposit as a function of time; P_S=5.5×10^4 $W cm^{-2}$; acquisition time:0.5 s, interval:1 s

All spectra of the series presented thereafter were thus normalized with regards to their respective area after a linear baseline subtraction in order to specifically highlight the chemical enhancement (CE) processes. The SERS intensities obtained using an acquisition interval of 1 s are presented in Figure 3, in which the coordinates are time and wavenumber.

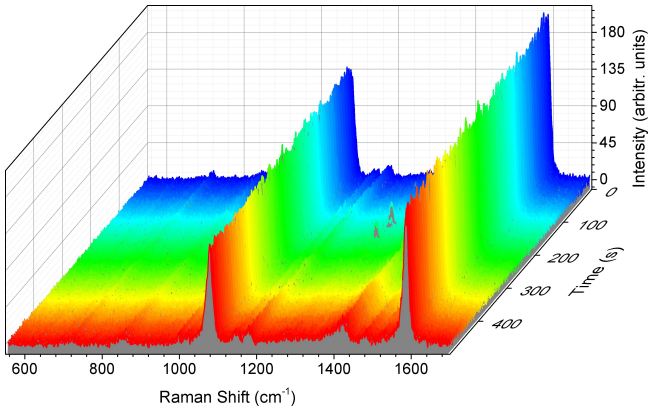

Fig. 3 Normalized SER spectra of MBA:Au deposit; P_S=5.5×10^4 $W cm^{-2}$; acquisition time:0.5 s, interval:1 s

The main peaks of MBA:AuNPs SERS, namely observed at 1587, 1078, 1422 cm^{-1} and, at a minor extend, 1480, 1178, and 1143 cm^{-1} are observed in all spectra presented in Figure 3. In addition to this main signal, some spectra individually feature original profile, which look fully reversible. In particular, the SER spectra recorded at 157 and 197 s exhibit additional lines around 1290 and 1500 cm^{-1}†. Non-reversible changes also occurred: the intensities of both Raman peaks detected at 997 and 1021 cm^{-1} as well as the contribution at 1570 cm^{-1} irreversibly increased with time according to a first-order reaction rate, as is refined in Figure 4. In return, the intensity of the bands located at 1078, 1422 and

* The area variation of the series recorded at $P_S = 6 \times 10^3$ $W cm^{-2}$ is presented in supporting information

† A contour plot corresponding to the same experiment is presented in Supporting Information

1587 cm^{-1} were found to decrease with the same rate constant, indicating that a share of the probed adsorbed p-MBA molecules has been decarboxylated to form mono-substituted species.

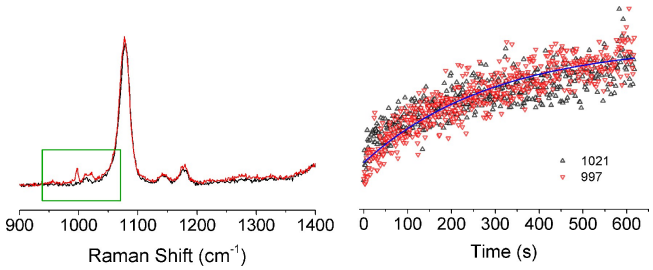

Fig. 4 left: Normalized first (black) and last (red) SER spectra; right: evolution with time of the intensities at 997 and 1021 cm^{-1}; P_S=5.5 × 10^4 W cm^{-2};

In order to have a global picture of the way the spectral trends evolve, either in a synchronized manner or not, we have calculated the correlation matrix built with the covariance values $\sigma(\bar{\nu_n},\bar{\nu_m})$ crossing the the intensities $I_i(\bar{\nu_n})$ and $I_i(\bar{\nu_m})$ of the SERS signal recorded at $t = i$ for the two wavenumbers $\bar{\nu_n}$ and $\bar{\nu_m}$, respectively.

$$\sigma(\bar{\nu_n},\bar{\nu_m}) = \frac{1}{N}\sum_i[(I_i(\bar{\nu_n}) - \langle I(\bar{\nu_n})\rangle) \times (I_i(\bar{\nu_m}) - \langle I(\bar{\nu_m})\rangle)] \quad (1)$$

$\langle I(\bar{\nu_n})\rangle$ and $\langle I(\bar{\nu_m})\rangle$ are the expected values of the SERS intensity at $\bar{\nu_n}$ and $\bar{\nu_m}$, respectively. The resulting correlation map is presented in Figure 5 in the form of a contour plot. Negative covariance values give dark blue traces whereas positive values are gradually represented by green ($\sigma(\bar{\nu_n},\bar{\nu_m})$=1) to red ($\sigma(\bar{\nu_n},\bar{\nu_m})$>11) regions.

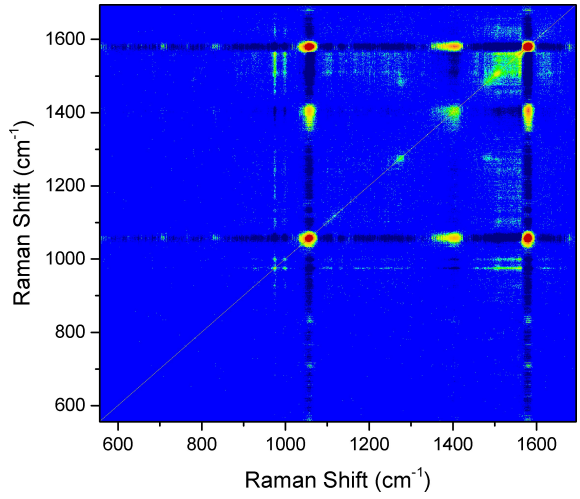

Fig. 5 Covariance map of SER intensity variations . The spectral intensities were normalized by the area of each spectrum after baseline subtraction. P_S=5.5 × 10^4 W cm^{-2}

Two groups of peaks occurring competitively can be defined from Figure 5. The first group, further denoted as Group I for conciseness, is composed by the modes of AuNP:p-MBA detected at 721, 851, 1012, 1078, 1143, 1422 and 1587 cm^{-1}. This trend makes it clear that, on average, the intensities of the main peaks assigned to adsorbed p-MBA evolve simultaneously, as was already reported in the liquid phase by Zhang *et al.*[23]. The second group gathers the peaks previously assigned to decarboxylation products (997, 1022 and 1571 cm^{-1}) together with contributions observed around 1283, 1296, 1501 and 1522 cm^{-1}. The latter is correlated to the signature of decarboxylated species with a covariance value, $\sigma_{997,1522}$, of 2.4. On the other hand, the coloured spots visible at 1283, 1296 and 1501 cm^{-1} are not clearly positively correlated to other spectral features. Figure 6 shows the SERS intensity at 1283, 1296 and 1500 cm^{-1} as a function of time in the form of scatters together with a tentative representation of the occurrence of exceptionally high intensity values.

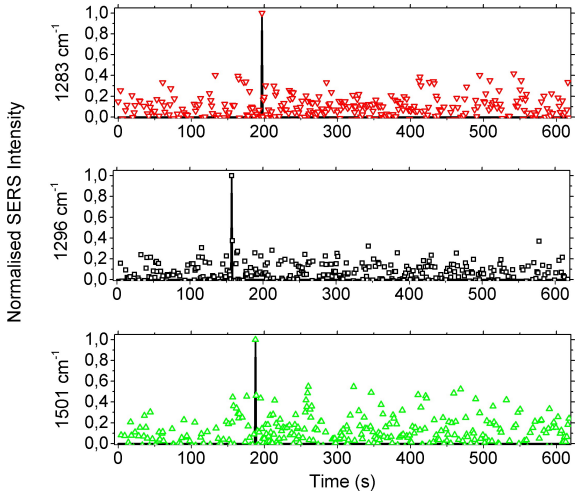

Fig. 6 SERS Intensity detected at 1283, 1296 and 1501 cm^{-1} as a function of time and corresponding ON-OFF behaviour

The "ON" state was decided for signals overcoming an arbitrary threshold of $2\sigma^2$ above the noise level and is represented by a vertical line in Figure 6. This analysis made it possible to observe that, according to the threshold we have used, only one spectrum of the whole series showed an exceptional intensity value for each of the three modes. In the following, the occurrence of such isolated features will be thus denoted as *individual events*. A selection of SER spectra corresponding to so-called *individual events* is presented in Figure 7.

In comparison with the initial spectrum, the key additional features are mainly located in the 1250-1305 cm^{-1} region. A peak which wavenumber varies from 1276 to 1298 cm^{-1} seems to randomly arise in several highlighted spectra. A similar band was observed by Kudelski in the SER spectra of p-MBA solutions in buffered medium after being adsorbed onto a roughened silver substrate for pH values ranging from 2 to 12.5[22]. Moreover, this mode is also found in bulk p-MBA or dimeric species[31] and can be assigned to an *in-plane* CH bending+CC stretching vibration (ν_{14}) having a B_2 symmetry. The *individual events* observed during the Series typically feature a lifetime corresponding to 1 spectral acquisition (0.5 s) and neither coincided with any spectral enhancement of the whole SER intensity nor an increase of the

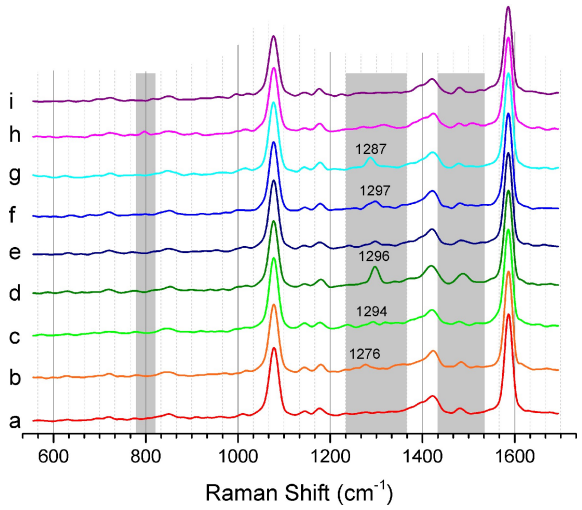

Fig. 7 SER spectra corresponding to individual events recorded at a) 1 s (reference), b) 45 s, c) 117 s, d) 157 s, e) 164 s, f) 165 s, g) 197 s, h) 267 s and i) 529 s; acquisition time: 0.5 s, interval: 1 s; P_S=5.5 × 10^4 W cm^{-2}

background level‡.

The time range of our SERS acquisition is not consistent with the the observation of chemical intermediates, which characteristic lifetime is expected to be shorter by several orders of magnitude. In a context of single molecule detection, mild fluctuations of SERS intensity were related to the diffusion dynamics of the molecule on the solid surface and were proposed by Bizzarri *et al.* to be likened to a random walk following a Lévy statistics[16]. Alternatively, the modification of the close environment of the molecule can also lead to transient resonant structures and, thus, produce a gate opening of different vibrational modes.

3.2.3 Statistical investigation of so-called individual spectra as a function of the specific power

In general, individual events can be refined by means of the excess Kurtosis coefficient $\gamma_2(\bar{\nu})$ defined for each Raman Shift over time by:

$$\gamma_2(\bar{\nu}) = \frac{\mu^4(\bar{\nu})}{\sigma^4(\bar{\nu})} - 3 \qquad (2)$$

where μ^4 is the fourth moment about the mean and σ is the standard deviation. The Kurtosis coefficient describes the propensity of a given system to produce outliers. In the present case, a high Kurtosis value reflects the combination of (i) a high degree of abnormality of the SERS signal and (ii) a significant contribution of the new signal. In other words, the long-range temporal evolutions and the experimental noise are discarded from this description, which is not only an amplification of SER signal. The use of the excess Kurtosis descriptor makes it possible to get a qualitative description of extreme events without requiring a time filter, as was the case for the analysis of q-residuals[17]. Figure 8 presents the values of excess Kurtosis coefficient as a function of the wavenumber for increasing specific power at the sample.

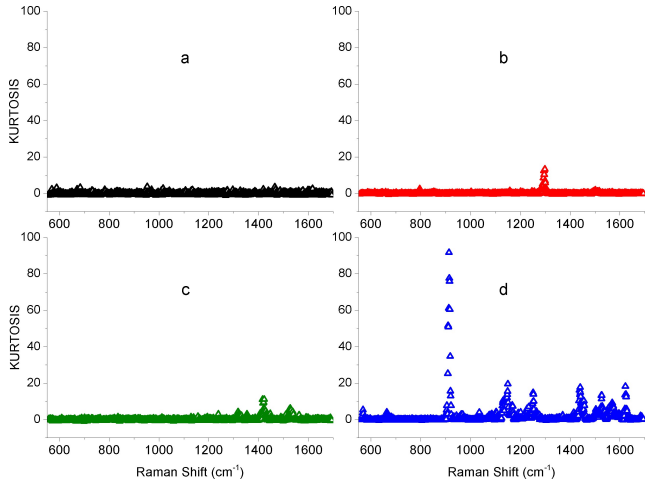

Fig. 8 Value of Kurtosis as a function of wavenumber afforded from SERS spectra recorded with a specific power of a) 6 × 10^3 W cm^{-2}, b) 5.5 × 10^4 W cm^{-2}, c) 1.0 × 10^5 W cm^{-2} and d) 2.3 × 10^5 W cm^{-2}

From the data presented in Figure 8, it is visible that the specifically enhanced vibration modes are different from one series to another. Repeating the very same experiment made it possible to clarify that there is no particular correlation between the characteristic wavenumbers of the individual events and the laser power applied. However, the spectral enhancement does not seem to occur fully randomly with wavenumber: only a finite number of spectral regions are prone to signal enhancement. As a first attempt to bring some hints to this hypothesis, Figure 9 gathers the Kurtosis profiles over wavenumbers obtained along 15 experiments run with specific powers of 5.5 × 10^4 W cm^{-2} and 1.0 × 10^5 W cm^{-2}.

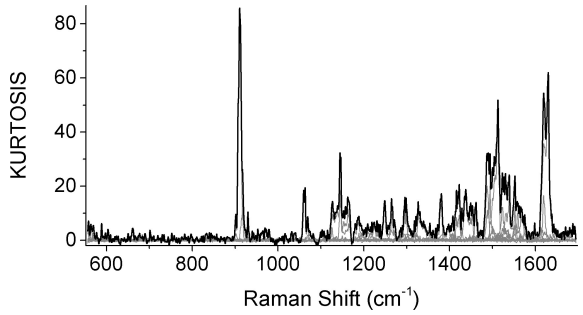

Fig. 9 Kurtosis values as a function of wavenumber obtained from 15 independent experiments (grey lines) and sum of all Kurtosis values

On the base of a Series of 15 experiments gathering around 9000 spectra presented in Figure 9, several modes appear as being prone to transient enhancement, while other wavenumbers, located in the 600-800 cm^{-1} region for example, do not show any exceptional intensity value. In the present case, our results suggest that the black curve in Figure 9 illustrates a spectral channel of independent modes which ON/OFF behaviour produced the *individual events* we have observed. This "wavenumber comb" exhibits gates in the 900-1650 cm^{-1} region, which can be assignable to Raman-active modes of isolated p-MBA molecule

‡ A Figure aiming at supporting this specific observation is presented in Supporting information

on the base of theoretical calculations provided by Li *at al.*[24]. More precisely, the fragments we have transiently detected mainly involved thiol groups ($\sim$910 cm^{-1}), carbonyl bonds ($\sim$1620 cm^{-1}) and ring modes having a B_2 symmetry. Upon adsorption onto silver or gold nanoparticles, the thiol groups of p-MBA are expected to form stable thiolate bonds[29]. Hence, we propose that the *individual events* are due to the transient detection of a fragment of single p-MBA molecule belonging to the second coordination layer.

Finally, it is visible from Figure 8 that, for a given duration of spectral acquisition, the number of individual events giving rise to exceptional γ_2 values increases with the specific power at the sample. For example, let us consider the number of occurrences of $\gamma_2 > 3.5$ in 10 minutes, which is 6 times higher than the noise level in the most noisy case of P_{laser}=6 $\times$ 10^3 W cm^{-2} (Figure 10). On that note, the maximal value of Kurtosis as a function of the specific power applied follows a similar trend, as is presented in Supporting Information.

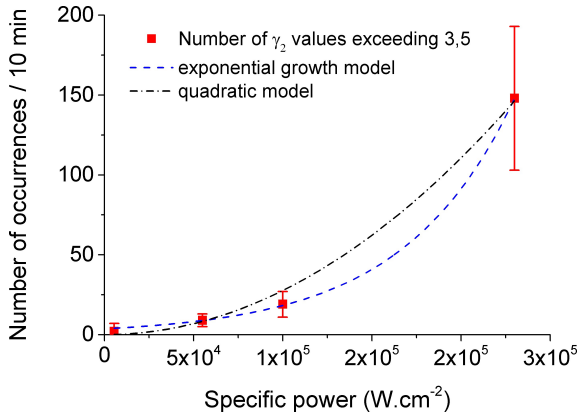

Fig. 10 Number of occurrences of γ_2 values exceeding the value of 3.5 during 10 minutes of spectral acquisition as a function of the specific power applied

It is clear that the number of exceptionally original SER spectra features a non-linear dependence to the specific power applied. This observation suggests that the enhancement process is photothermally activated. More precisely, we propose that increasing the laser power produced a more pronounced heat dissipation in the very vicinity of the nanostructure[28] and induced a Brownian motion-driven local re-organization AuNPs surfaces at nanometric scale. The time range for heat dissipation and the induced Brownian motion of AuNPs in the analysed confocal volume is, this time, compliant with the temporal resolution of our analysis. Following this hypothesis, resonant structures allowing an efficient charge transfer involving the second coordination sphere could reversibly occur within a time range of one second and produce an *individual event*. The re-organisation of plasmonic surfaces upon external heating was demonstrated in the extreme case of non-reversible nanoparticle sintering by Kho *et al.*[32] while laser-induced nanoparticles Brownian motion in water was described by Rings *et al.*[33], giving substance to the present hypothesis. It is also to be noticed that the absence of enhancement decay in the experimental data we present here suggests that the gold nanoparticles were not subject to coalescence. Moreover, taking into account the very local and transient character of CE mechanisms involved in the *individual events*, no non-reversible evolution in the nanoparticles deposit morphology is expected to be observable using up-to-date imaging techniques.

4 Conclusion

Our results prove that it is possible to refine both electromagnetic and chemical enhancements from a series of SER spectra by using the Kurtosis descriptor, the time-evolution of reaction products characteristic lines and the covariance values in a complementary manner. Providing that the acquisition time is short enough, few individual events which are not directly correlated to each other are observed. The number of occurrences of these individual events was shown to non-linearly increase with the specific power applied. We have proposed that *individual events* are due to a transient SERRS phenomenon allowed by the thermally-activated formation of particular local resonant structures. Thus an efficient charge-transfer process made it possible to observe fragments of molecules belonging to the second layer of p-MBA.

Acknowledgements

We thank the University of Edinburgh for supporting the 1-year research stay of Gina Smith at UCCS. Pr. Pierre Suret is acknowledged for discussions about the statistical description of extreme events.

References

1 M. Moskovits, *Rev. Mod. Phys.*, 1985, **57**, 783.
2 K. Kneipp, Y. Wang, H. Kneipp, L. T. Perelman, I. Itzkan, R. R. Dasari and M. S. Feld, *Phys. Rev. Lett.*, 1997, **78**, 1667.
3 M. L. Brongersma, N. J. Halas and P. Nordlander, *Nature Nano.*, 2015, **10**, 25–34.
4 E. M. van Schrojenstein Lantman, O. L. J. Gijzeman, A. J. G. Mank and B. M. Weckhuysen, *ChemCatChem*, 2014, **6**, 3342–3346.
5 C. Novo, A. M. Funston and P. Mulvaney, *Nature Nano.*, 2008, **3**, 598–602.
6 C. E. Harvey and B. M. Weckhuysen, *Catal. Lett.*, 2015, **145**, 40–57.
7 J. Gersten and A. Nitzan, *J. Chem. Phys.*, 1980, **73**, 3023–3037.
8 M. Thomas, S. MÃijhlig, T. Deckert-Gaudig, C. Rockstuhl, V. Deckert and P. Marquetand, *J. Raman Spectrosc.*, 2013, **44**, 1497–1505.
9 P. Kambhampati, C. Child, M. C. Foster and A. Campion, *J. Chem. Phys.*, 1998, **108**, 5013–5026.
10 N. Valley, N. Greeneltch, R. P. Van Duyne and G. C. Schatz, *J. Phys. Chem. Lett.*, 2013, **4**, 2599–2604.
11 A. Kudelski and B. Pettinger, *Chem. Phys. Lett.*, 2004, **46**, 76–79.
12 J. Wang, M. McEntee, W. Tang, M. Neurock, A. P. Baddorf, P. Maksymovych and J. T. Yates, *J. Am. Chem. Soc.*, 2016, **138**, 1518–1526.

13 A. Szeghalmi, S. Kaminskyj, P. Rösch, J. Popp and K. M. Gough, *J. Phys. Chem. B*, 2007, **111**, 12916–12924.

14 A. Kudelski, *J. Raman Spectrosc.*, 2007, **38**, 1494–1499.

15 A. R. Bizzarri and S. Cannistraro, *Phys. Chem. Chem. Phys.*, 2007, **9**, 5315–5319.

16 A. R. Bizzarri and S. Cannistraro, *Phys. Rev. Lett.*, 2005, **94**, 068303.

17 E. M. van Schrojenstein Lantman, P. de Peinder, A. J. G. Mank and B. M. Weckhuysen, *ChemPhysChem*, 2015, **16**, 547–554.

18 A. Michota and J. Bukowska, *J. Raman Spectrosc.*, 2003, **34**, 21–25.

19 K. L. Nagashree, R. Lavanya, C. Kavitha, N. S. Venkata Narayanan and S. Sampath, *RSC Adv.*, 2013, **3**, 8356–8364.

20 Y. Zong, Q. Guo, M. Xu, Y. Yuan, R. Gu and J. Yao, *RSC Adv.*, 2014, **4**, 31810–31816.

21 C.-H. Ho and S. Lee, *Colloids Surf. A*, 2015, **474**, 29 – 35.

22 A. Kudelski, *J. Raman Spectrosc.*, 2009, **40**, 2037–2043.

23 Q. Zhang, Y. Yuan, C. Wang, Z. Zhou, L. Li, S. Zhang and J. Xu, *J. Raman Spectrosc.*, 2015, n/a–n/a.

24 R. Li, H. Lv, X. Zhang, P. Liu, L. Chen, J. Cheng and B. Zhao, *Spectrochim. Acta A*, 2015, **148**, 369 – 374.

25 M. Osawa, N. Matsuda, K. Yoshii and I. Uchida, *J. Phys. Chem.*, 1994, **98**, 12702–12707.

26 J. Ftouni, M. Penhoat, A. Addad, E. Payen, C. Rolando and J.-S. Girardon, *Nanoscale*, 2012, **4**, 4450–4454.

27 K. W. Kho, Z. X. Shen, H. C. Zeng, K. C. Soo and M. Olivo, *Anal. Chem.*, 2005, **77**, 7462–7471.

28 K. Ikeda, S. Suzuki and K. Uosaki, *J. Am. Chem. Soc.*, 2013, **135**, 17387–17392.

29 J. V. Maya Girón, E. Zelaya, A. Rubert, G. Benítez, P. Carro, R. C. Salvarezza and M. E. Vela, *J. Phys. Chem. C*, 2013, **117**, 24967–24974.

30 J. S. Suh and J. Kim, *J. Raman Spectrosc.*, 1998, **29**, 143–148.

31 J. Gao, Y. Hu, S. Li, Y. Zhang and X. Chen, *Spectrochim. Acta A*, 2013, **104**, 41–47.

32 K. W. Kho, Z. X. Shen, Z. Lei, F. Watt, K. C. Soo and M. Olivo, *Anal. Chem.*, 2007, **79**, 8870–8882.

33 D. Rings, R. Schachoff, M. Selmke, F. Cichos and K. Kroy, *Phys. Rev. Lett.*, 2010, **105**, 090604.